Magnetic mineralogy in Barranca Tlalpan exposure paleosols, Tlaxcala, Mexico

Beatriz Ortega-Guerrero[1,*], Sergey Sedov[2], Elizabeth Solleiro-Rebolledo[2], and Ana Soler[1]

[1] Instituto de Geofísica, [2] Instituto de Geología
Universidad Nacional Autónoma de México, Cd. Universitaria, 04510 México D.F., Mexico
** bortega@tonatiuh.igeofcu.unam.mx*

ABSTRACT

The knowledge of past climatic and environmental conditions in central Mexico, interpreted extensively from lacustrine records, is restricted to the last ca. 50,000 years. The recent discovery of new localities of paleosol sequences in central Mexico and the reconnaissance of their usefulness as records of environmental change provides a new source of information about past climatic conditions for times prior to the last full glacial. In this paper, we analyze the mineral magnetic properties of a sequence of paleosols developed in volcaniclastic deposits and evaluate these data as paleoenvironmental proxy. The sequence consists of a modern Phaeozem soil and seven late Quaternary Luvisol paleosols outcropping in Barranca Tlalpan, Tlaxcala, Mexico. Rock magnetic analysis was used to study the concentration and type of magnetic mineralogy. The mineral magnetic data, supported by soil morphological and chemical data, are interpreted to indicate that the paleosols can be grouped in three sets, each with distinct characteristics. The Red set paleosols P7 and P6 are the most weathered, and present the highest magnetic concentration composed of Ti-magnetite and ultrafine magnetite (<30 nm). The Brown set of paleosols P5, P4 and P3, with few redoximorphic features, have coarser grains and lower concentrations of magnetic minerals. The Gray set, paleosols P2 and P1, have abundant redoximorphic features including Fe–Mn nodules, and have a multicomponent magnetic mineralogy of coarse size. Paleosols from the Red and Brown sets conserve evidence of neoformation of ultrafine magnetite grains in the Bt horizons, probably derived from pedogenic processes. However, direct observations by microscopy and rock magnetism parameters point to a later destruction of this ultrafine fraction. We consider that even if pedogenic processes resulted in the formation of ultrafine magnetite, redoximorphic conditions under humid climates are responsible of the destruction of magnetic minerals. Such conditions may have strongly prevailed in the Gray set paleosols, whereas the Red set was probably developed under contrasting seasonal precipitation climates, which favored the formation and preservation of pedogenic magnetic minerals.

Key words: paleosols, rock magnetic analysis, central Mexico.

RESUMEN

El conocimiento sobre las condiciones paleoclimáticas y paleoambientales en la parte central de México, derivadas de registros de sedimentos lacustres, se restringen a los últimos 50,000 años. El reciente descubrimiento de secuencias de paleosuelos en el centro de México, y el reconocimiento de su utilidad como registros de cambios ambientales, proporcionan una nueva fuente de información sobre condiciones climáticas anteriores al último glacial. En este trabajo, presentamos los resultados del análisis de las propiedades magnéticas de minerales de una secuencia de paleosuelos, desarrollada en depósitos volcaniclásticos, y evaluamos estos datos como registros indicadores de paleoambientes. La secuencia estudiada consiste de un suelo moderno Phenozem, y siete paleosuelos Luvisol del Cuaternario

tardío, que afloran en la Barranca Tlalpan, Tlaxcala, México. Los análisis de magnetismo de rocas fueron utilizados para determinar la concentración y el tipo de minerales magnéticos presentes. De acuerdo a los resultados de la mineralogía magnética, sustentados por datos geoquímicos y de morfología de suelos, los paleosuelos pueden agruparse en tres unidades, cada una de ellas con características distintivas. La unidad Roja, que abarca los paleosuelos P7 y P6, presenta el mayor grado de intemperismo, y la mayor concentración de minerales magnéticos, compuestos por titanomagnetita y magnetita ultrafina (<30 nm). La unidad Parda, que comprende los paleosuelos P5, P4 y P3, presenta escasas características redoximórficas, contiene granos de mayor tamaño y concentraciones menores de minerales magnéticos que la unidad Roja. La unidad Gris, que incluye los paleosuelos P2 y P1, contiene abundantes rasgos redoximórficos, incluyendo nódulos de Fe–Mn, y tiene una minerolgía magnética multicomponente de grano grueso. Los paleosuelos de las unidades Roja y Parda conservan evidencias de la neoformación de granos ultrafinos de magnetita en los horizontes Bt, probablemente derivados de procesos pedogénicos. Sin embargo, observaciones directas al microscopio y los parámetros de mineralogía magnética, indican una posterior destrucción de esta fracción ultrafina. Consideramos que, aún si los procesos pedogénicos dieron por resultado la formación de magnetita ultrafina, las condiciones redoximórfcas bajo climas húmedos son responsables de la destrucción de los minerales magnéticos. Estas condiciones pudieron haber permanecido durante la formación de los paleosuleos de la unidad Gris, en tanto que la unidad Roja probablemente se desarrolló bajo climas con una precipitación estacional contrastante, los cuales favorecieron la formación y preservación de minerales magnéticos pedogénicos.

Palabras clave: paleosuelos, análisis de magnetismo de rocas, centro de México.

INTRODUCTION

Rock magnetic methods have been successfully applied in paleoclimatic reconstruction (*e.g.*, Reynolds and King, 1995) in a great variety of sedimentary environments, as climate has a great effect on sedimentation and weathering processes that affect the resulting magnetic mineral assemblages. Magnetic properties in soils depend not only on minerals inherited from parent materials, but on pedogenic processes such as weathering and biogenic mineral neoformation.

Since discovery of the enhancement of magnetic susceptibility in paleosols compared to loess (Kukla, 1988), the mineral magnetic record of Chinese loess–paleosol sequences has been extensively studied, providing one of the longest continental climate records covering the last 2.5 Ma. It was found that pedogenic processes are responsible for the formation of fine-grained magnetite and maghemite (Maher and Thompson, 1991), and this enhancement has provided a proxy for paleoprecipitation (Maher and Thompson, 1995). However, such magnetic enhancement is not present in the soils of loess–paleosol sequences from some other regions (Bèget, 1990); thus this does not constitute a universal proxy of paleo-rainfall.

The mechanisms that result in the *in-situ* formation of magnetic minerals in soils are not fully understood. Dearing *et al.* (1996) summarize the causes of the presence or enrichment of magnetic minerals in soils as: long-term weathering that concentrate residual primary magnetic minerals (Singer and Fine, 1989), biotic formation of fine-grained magnetite or greigite by bacteria (Lovely and Philips, 1986; Fassbinder *et al.*, 1990; Stanjek *et al.*, 1994), fire-induced transformation of weak magnetic iron oxides and hydroxides into magnetite or maghemite (Le Borgne, 1960; Kletetschka and Banerjee, 1995), and airborne magnetic pollution particles (Thompson and Oldfield, 1986). From a study of a set of modern soils, Dearing *et al.* (1996) conclude that abiological weathering of Fe-bearing minerals, which result in the formation of ferrihydrite, and a later bacterial reduction to magnetite, which can later oxidize to maghemite, are the causes of the formation of secondary ultra-fine grains of ferrimagnetic minerals.

In Czech loess–paleosol sequences, Oches and Banerjee (1996) found that magnetic enhancement depends on the degree of pedogenesis and the type of paleosols, and they also found a good correlation between magnetic parameters and paleoclimate. However, for the soils from the full interglacial, with the warmest and most humid conditions, iron resided in antiferromagnetic minerals such as hematite, which could suggest a long-term oxidation of magnetite to hematite. Mineral magnetic analysis, thus, does not constitute *per se* a proxy of climatic change, as magnetic properties can be the result of a sum of different processes whose interpretation is not unique. For this reason, it is necessary to compare magnetic parameters with soil morphological and chemical data to provide a valid model of past environmental conditions. Contrary to the loess–paleosol sequences, there is rather restricted knowledge of the magnetic properties of paleosols derived from other parent materials, including those of volcanic origin. Recently, the tephra–paleosol sequences of the Transmexican Volcanic Belt were recognized as a valuable record of the late Quaternary environmental change (Sedov *et al.*, 2001), thus putting forward the question: can paleosol magnetic

minerals be utilized as paleoclimate proxy? As a first attempt to resolve this question, we investigated a sequence of toba–paleosols in Barranca Tlalpan, central Mexico. Here we present the initial results of a major mineral magnetic research in volcaniclastic sequences, and compare the obtained results with geochemical and mineralogical data, in order to estimate the potential usefulness of magnetic data in the paleoclimatic reconstruction of the studied exposure.

SETTING

The toba–paleosol sequence is located in Barranca Tlalpan, 15 km north–northwest from Tlaxcala city. A barranca is a deep gully cut by running water. The exposed sequence contains seven pedostratigraphic units that are separated by indurated volcanic ash layers (toba sediments) (Figure 1).

Soil–paleosol sequence

Four morphologically different units are separated within Tlalpan profile:

1) Late Holocene Anthropic Phaeozem (S1) consists of gray-brown loamy Ah horizon with subangular blocky structure, containing abundant artifacts (*e.g.*, ceramic fragments, obsidian tools). It is separated from the AB horizon of the underlying unit P1 by an abrupt boundary. Down the slope, the Anthrosol merges into a ~5m thick colluvial stratum with at least 2 buried incipient Ah horizons –the product of human-enhanced erosion caused by pre-Hispanic land use.

2) Paleosols P1 and P2 are separated by a cemented Cm horizon (tepetate). Both paleosols have Bt horizons characterized by pale gray colour, well developed subangular blocky-prismatic structure and abundant redoximorphic features such as hard black rounded Fe–Mn concretions, ferruginous nodules, and mottles. In thin

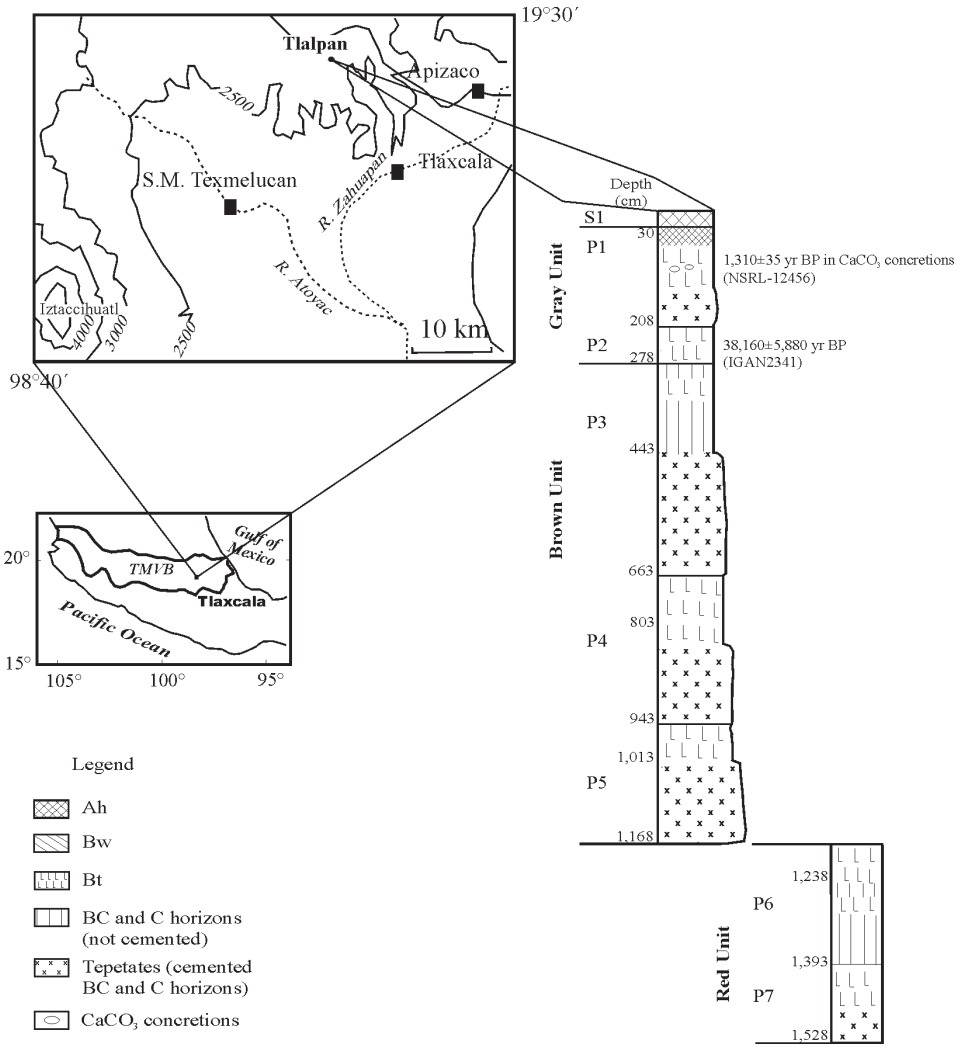

Figure 1. Location map of the Barranca Tlalpan, Tlaxcala, México, and stratigraphic section of Barranca Tlalpan exposure.

sections, illuvial clay coatings were observed in the Bt horizons in both P1 and P2. Bt horizons show elevated clay content, up to 50% in P2, but strikingly low quantities of dithionite-citrate-bicarbonate (DCB) extractable iron: 0.2–0.3%, probably due to iron migration and segregation caused by redoximorphic processes. Unexpectedly, neoformed carbonates were found in these paleosols: hard concretions in the Bt horizons of P1 and mostly vermicular forms and pseudomicelium below. No primary carbonates are present in the matrix. We found small Fe–Mn concretions included in some of the carbonate concentrations. This suggests that carbonate neoformation occurred after the stage of leaching, clay illuviation, and redoximorphic processes. Paleosols of this group were defined as Gleyic Luvisols. The paleosols P1 and P2 are grouped as the 'Gray' set.

3) Paleosols P3, P4 and P5, consist of well-developed Bt horizons that are underlain by hard and indurated Cm horizons –tepetates– ('Brown' set). Both Bt horizons and tepetates have brown colour. Bt horizons are characterized by well-developed subangular blocky structure and abundant illuvial clay coatings on ped surfaces, observed both macromorphologically and in thin section. Redoximorphic features –mostly Fe–Mn mottles and coatings on ped surfaces– are less frequent than in PT1 and PT2. Clay content in Bt horizons varies in the range 27–40%, and DCB extractable iron from 0.5 to 1%. These paleosols are classified as Haplic Luvisols.

4) The lowest paleosols in the sequence, P6 and P7, have Bt horizons of intensive brown-red colour ('Red' set). P6 is a pedocomplex, consisting of 2 well-developed Bt horizons (P6 and P6a), and is underlain by a relatively thin BC horizon. Paleosol P7 has the thickest Bt horizon, and is underlain by the basal sandy tepetate (Cm) layer. Well-developed thick illuvial clay coatings are present in these paleosols; observations in thin sections showed that in paleosol P7 they are partly fragmented and incorporated in the matrix as clay papules. All paleosols of the Red set are characterized by relatively high accumulation of clay (about 50%) and DCB-extractable Fe_2O_3 (1.2–1.4 %). These paleosols are classified as Chromic Luvisols.

Petrographic study of thin sections showed that the sand and silt fractions of the paleosol parent material (BC and Cm horizons) consist mostly of pyroclastic components: plagioclase, pyroxene, amphibole, volcanic glass, and few opaque minerals. In the paleosol Bt horizons all these minerals have various weathering features, which are most strong in the Red set.

Age of paleosols

The presence of numerous pre-Hispanic artifacts indicates that the surface Anthric Phaeozem has a maximum age of about 2,500 yr BP. The ^{14}C age of humus in paleosol P2 is 38,160±5,880 yr BP, meaning that the period of formation of P1 extends over at least oxygen isotope stage (OIS) 2 and the major part of the Holocene. One Accelerator Mass Spectrometry (AMS) date on carbonate from hard concretions is just 1,310±35 yr BP, favoring the micromorphological interpretation that carbonate neoformation occurred in the latest phase of pedogenesis, after the period of leaching, clay illuviation, and redoximorphic processes. We speculate that neoformation occurred in the late Holocene in response to aridisation and/or changes in water balance associated with the beginning of surface Anthrosol formation.

No analytical dates are available at present to determine the age of the paleosols P3–P7. However, assuming that more than 10,000 years are needed in most cases for a well developed Bt horizon to form (Birkeland, 1984, 1992), we conclude that the formation of the sequence occurred over a period of at least 100,000 yr.

METHODS

Representative sampling was done in every soil horizon, by cutting a block of roughly 12x10x7 cm, and homogenizing it in the laboratory. Forty-seven samples from seven paleosols and one modern soil were taken. For rock-magnetism analyses, three subsamples of each sample were collected in 8 cm^3 plastic cubes. Curie temperature estimations were performed on a Bartington MS2WF furnace system, in which changes in magnetic susceptibility (χ) were measured from 25º to 650º C, during heating and cooling, in air. Low temperature (10–300 K) remanence measurements were done on selected samples in a Quantum Designs MPMS2 SQUID magnetometer. A field of 2.5 Tesla (T) was applied at room temperature, and cooled to 10 K (cooling curves) in zero field; a 2.5 T field was imparted at this temperature again, and remanences measured while warming to room temperature (warming curves) in zero field. Susceptibility and remanence measurements were done on all subsamples and results presented are the average value of the three measurements; saturation and coercivity parameters were only performed in one subsample of the set. Mass specific low-field magnetic susceptibility (χ) was measured in a Bartington system. Frequency dependence of susceptibility was measured in frequencies of 0.465 (χ_{lf}) and 4.65 (χ_{hf}) kHz, and calculated as $\chi_{fd\%} = (\chi_{lf}-\chi_{hf})/\chi_{lf}$. All remanences were measured in a Molspin Minispin fluxgate magnetometer. Anhysteric remanent magnetizations (ARM) were imparted in a 50 μT bias field, superimposed on a peak alternating field of 100 mT in a Schonstedt GSD-1 demagnetizer. Isothermal remanent magnetizations (IRM) were imparted with a pulse magnetizer at a forward field of 1 T and at backward fields of 100, 200 and 300 mT. The magnetization acquired at 1 T was considered the saturation magnetization (SIRM). The S ratio was calculated as $S = (IRM_{300}/SIRM)x100$, where SIRM is the value obtained at 1 T field and IRM_{300} the value obtained in the 300 mT backward field. Saturation magnetization (M_S) and

coercivity parameters B_{CR}, B_C, were obtained from hysteresis loops measured with a Princeton Measurement Corporation Micro-Vibrating Sample Magnetometer (μMag), and a Molspin Vibrating Sample Magnetometer (VSM), at room temperature in all samples. As the para-, dia- and ferrimagnetic fractions account for the χ, the ferrimagnetic susceptibility, χ_f, was calculated by subtracting the paramagnetic contribution estimated from the high field slope in the hysteresis loops from the bulk susceptibility.

In order to complement the magnetic mineralogy identification, and the estimations of magnetic mineral concentrations, we used a combination of non-magnetic techniques. Energy dispersive X-ray fluorescence analysis (XRF) for Ti and Fe, expressed as oxides, were carried out on the forty-seven samples. X-ray diffraction (XRD) in bulk samples was done only on samples with the highest magnetic susceptibility from the C and Bt horizons of paleosols P7 and P6. XRD analyses were performed by the powder method with a Brucker-axs D8-Advance. Extraction of magnetic minerals with a Franz electromagnet at 0.1 Ampere was conduced in samples of paleosol P7, from C and Bt horizon. The extracted material was used for reflected light microscopy (RLM), scanning electron microprobe observations (SEM) and energy dispersive X-ray analysis (EDAX).

RESULTS

Magnetic mineralogy

As a first approximation to the identification of the magnetic mineralogy, Curie temperature estimations were carried out as in all samples. Most of the warming curves present a continuous decay without sharp increases. Only a few show a weak inversion increase above 350° C (*e.g.*, P6 Bt1 sample, Figure 2) and are almost completely reversible even if the experiments were conducted in an air atmosphere (neither sealed capsules were used, nor an inert gas atmosphere was applied). Paleosol P7 is composed by two clear phases: the low Curie temperature phase is around 160° C, and the high Curie temperature phase is at 580° C. P6 samples mostly show a single phase and a drop near 580 °C. Curves from these Red set paleosols also display a drop in χ above 580 °C that continues until the maximum temperature, 650 °C, is reached. Paleosols P2 and P1 and modern soil S1 samples are very noisy, due to their magnetic weakness. In order to better observe the behavior of curves from these samples and to recognize their inflections, we applied a 6th-order polynomial fit to the data. The obtained curves of P2, P1 and S1, present a smooth decrease as temperature rises. However, changes in the slope at 60–

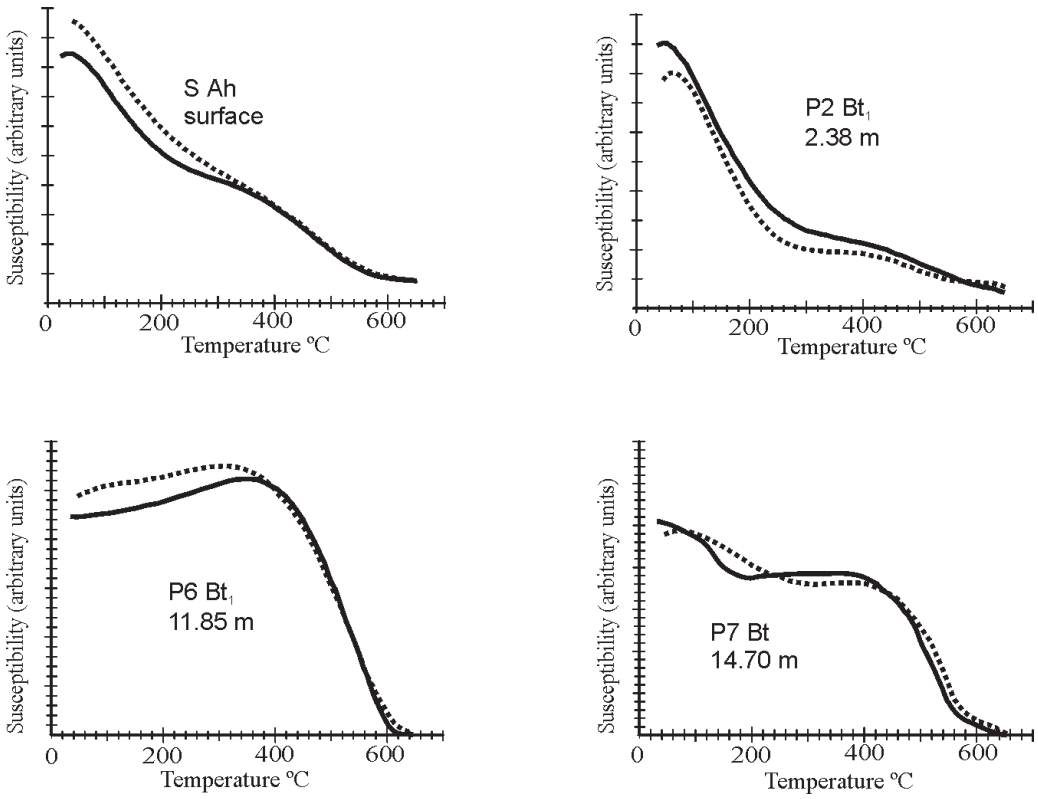

Figure 2. High temperature *vs.* susceptibility curves for selected samples. The depth of each sample in the exposure is indicated in meters. Solid line: warming curve; dashed line: cooling curves. Curie temperatures were estimated from these curves.

150°C, 200º–300° C and near 580° C can be observed in some samples (Figure 2). Paleosols P5, P4 and P3 show both types of curves exemplified by P6 and P7 in Figure 2. In S1, P1 (not shown), P2, P6, and P7 samples, a persistent decrease in susceptibility above 580° C is observed.

Pure magnetite has a Curie temperature close to 580°C. The content of Ti in titanomagnetite ($Fe_{3-x}Ti_xO_4$; $0 \leq x \leq 1$, represented as TM0–TM100) decreases the Curie temperature. A Curie temperature of 150º–200º C is typical of TM60, which is the primary Ti-magnetite in rapid cooled basaltic lavas. Hematite has a temperature of 675° C, however it is hard to detect because of its low magnetic signal that often is overwhelmed by the much stronger intrinsic magnetization of magnetite. The high content of paramagnetic minerals tends to present continuously decreasing curves, since their susceptibility varies inversely to the temperature.

All warming curves of low-temperature remanence

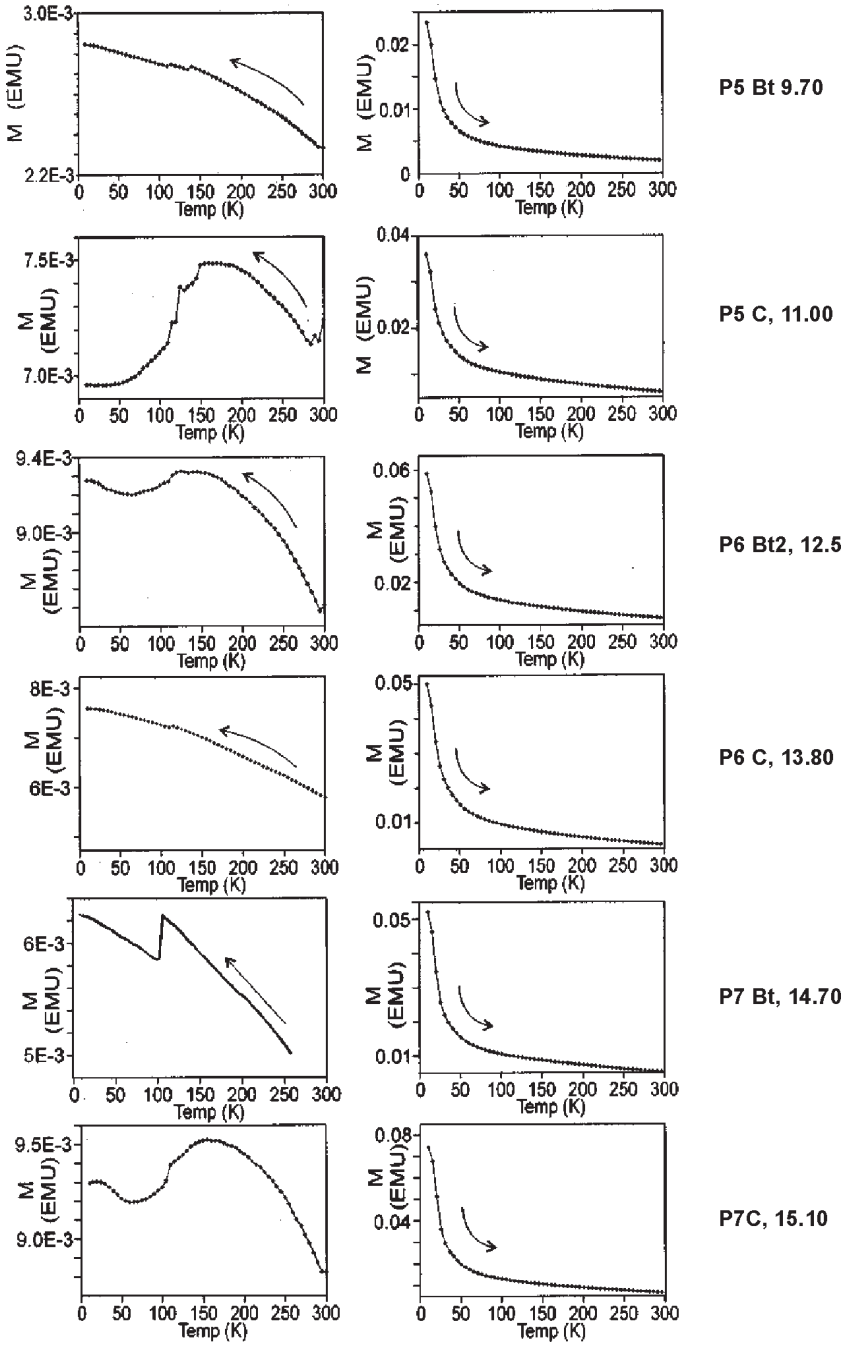

Figure 3. Low temperature demagnetization curves for selected samples of P5, P6, and P7 paleosols (numbers to the right of label are the sample depth in m). Curves to the left are the cooling experiments, and those to the right are the warming measurements.

measurements display a quick and large drop in remanence, very likely on account of the high superparamagnetic content that is thermally stable at 10 K (Figure 3). Cooling curves of P5 C, P6 Bt, and P7 C horizon samples exhibit a drop between ~145–120 K and ~60 K. This large drop occurs as the samples are cooled through the Verwey transition, which is a phase transition of magnetite that appears near 120 K (Özdemir *et al.*, 1993). Curves of P5 Bt, P6 C, and P7 Bt horizon samples show a steady increase in remanence while cooling, which could correspond to superparamagnetic (<0.03 μm) particles. Another possible interpretation for these curves is the presence of goethite (Dunlop and Özdemir, 1997). However, goethite has a Curie temperature near 120° C, which is hard to observe when high-Ti titanomagnetites are present.

Magnetic hardness of geological materials, the relative ease of a sample in acquiring a remanence in a backward field after saturation in a forward field (S ratios), is a useful guide in inferring high coercivity minerals. S_{300} ratios lower than 80% usually result from significantly high amounts of hematite or goethite. Lower S ratios in S1, P1 and P2 reflect high coercivity phases (Figure 4).

Ferrimagnetic contribution to susceptibility (χ_f) is higher than 95 % in most of the record, except in P2 and P1, where paramagnetic susceptibility (χ_p) varies from 6 to 17% (Figure 5). This indicates that paramagnetic material, such as clay, is significant in these gray paleosols.

From rock magnetism measurements, our best estimate of magnetic phases detected are titanomagnetites of a variable range of Ti content, from pure magnetite to TM70. Susceptibility data at high temperature and S ratios are consistent with high coercivity minerals (hematite or goethite) for S1, P1 and P2 samples. Low temperature χ behavior of P5 Bt, P6 C and P7 Bt samples might suggest the presence of goethite. However, the presence of goethite is one of the hardest assumptions to confirm by magnetic techniques, due to its weak magnetism and low thermal stability. Hematite content in P6 and P7 inferred from Curie temperature data is not supported by the high S ratios obtained.

XRD analyses were made on magnetic extracts from selected samples of the highest χ paleosols (P7). The concentration of magnetic minerals was too low, even in these samples, and consequently the quality of the X-ray scans is poor. For this reason, no further X-ray analyses were performed in the rest of the paleosols. XRD results obtained indicate the presence of magnetite and hematite as the only detected magnetic minerals. SEM observations

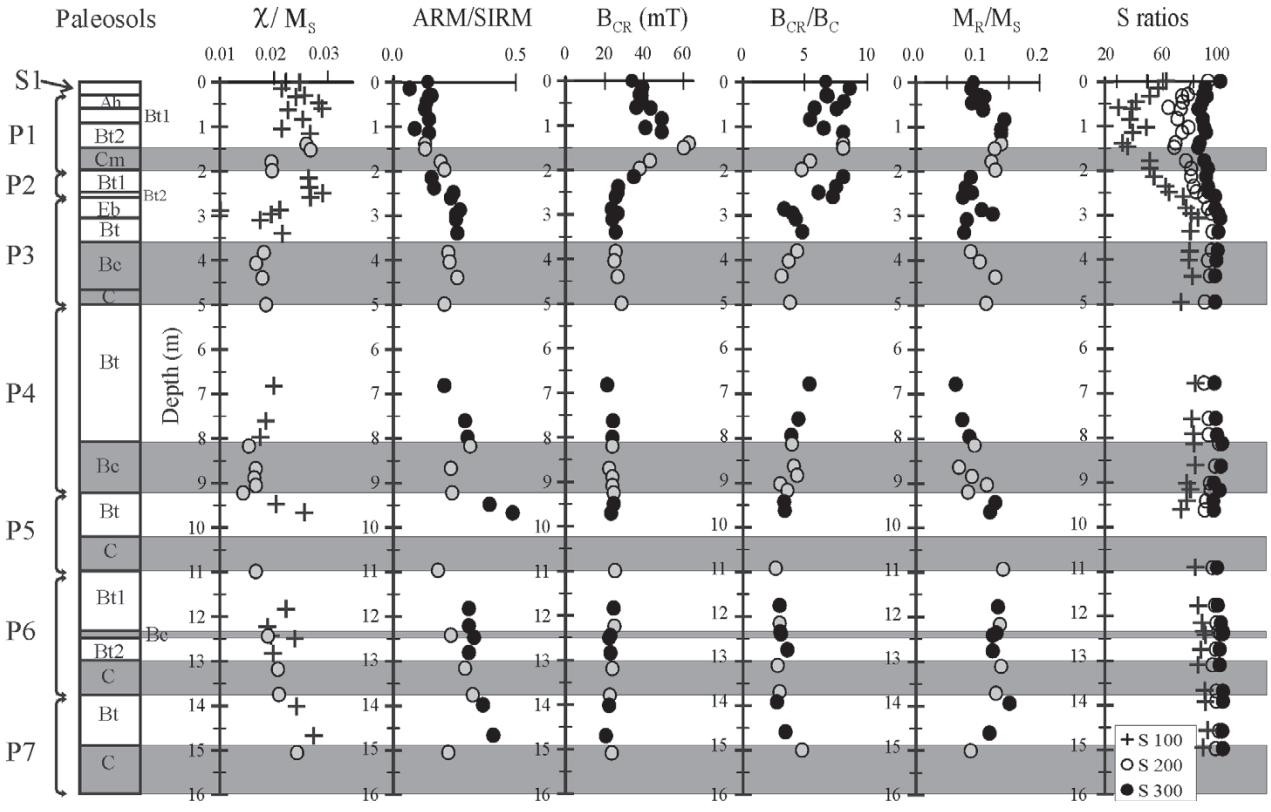

Figure 4. Depth profiles of magnetic hysteresis parameters and ratios. χ/M_S: Ratio of bulk susceptibility to magnetization of saturation, ARM/SIRM: anhysteric/saturation ratio of remanences; B_{CR}: coercivity of remanence; B_C: coercivity of saturation; M_R/M_S: remanence/saturation magnetizations ratio; S ratios: percentage of remanence growth in a backward field of 0.1 T (crosses), 0.2 T (open circles), and 0.3 T (black circles), after saturation of remanence in a 1T forward field. Open symbols on gray shaded areas correspond to samples from BC and C horizons.

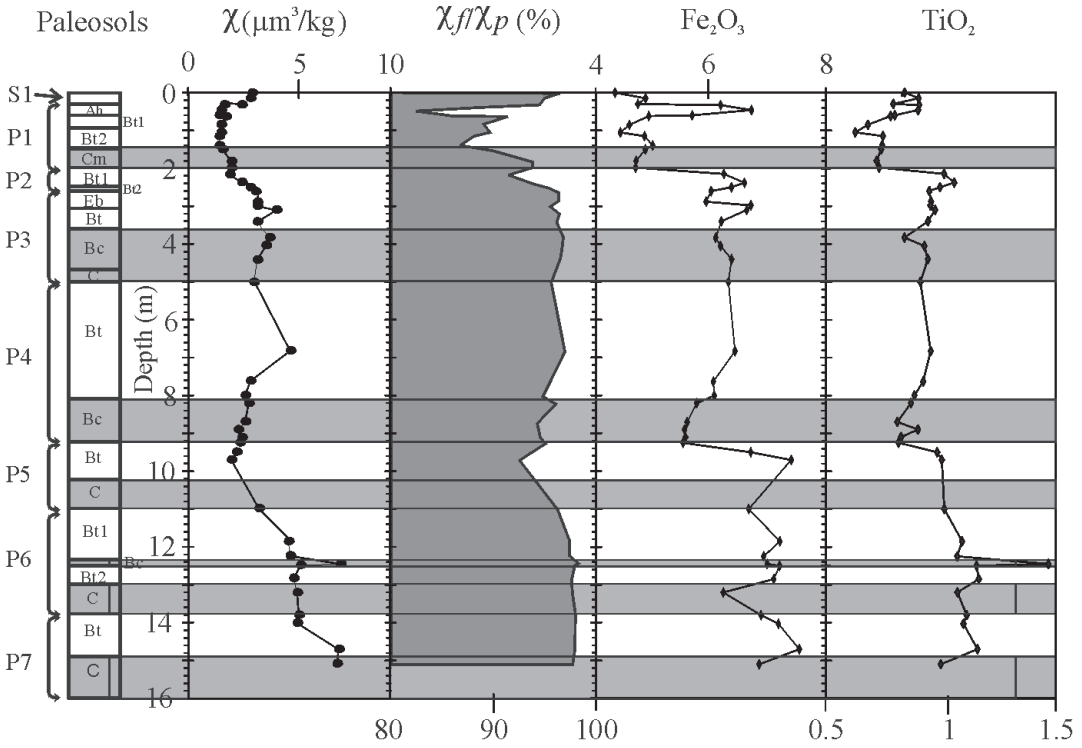

Figure 5. Magnetic susceptibility and some geochemical major oxides variations for Barranca Tlalpan exposure profile. χ: bulk magnetic susceptibility; χ_f/χ_p (%): ferrimagnetic, χ_f, contribution fraction to susceptibility, to paramagnetic, χ_p, fraction of susceptibility percentage. Major elements are given as weight percent of their oxides. Element concentrations were measured by X-ray fluorescence.

and EDAX analyses of magnetic separates show the dominance of Ti iron oxides. However, different grain morphology was observed in the two samples. The C horizon sample from P7 (15.10 m) generally presents ilmenite and Ti-magnetite grains less affected or unaffected by corrosion (Figure 6). The sample from the Bt horizon of P7 (14.70 m) has Ti-magnetite grains with corroded surfaces, which suggests that dissolution has occurred. RLM observations carried out in magnetic extracts of P7 Bt and P7 C horizon samples showed that Ti-magnetite and ilmenite with several degrees of hematization are the main iron oxides present in both samples. Hematite grains are also present, but in minor amount compared to Ti-magnetite and ilmenite. In both samples, scarce tiny grains of pyrite were found, which are thought to be of magmatic origin as they are included in quartz grains. Skeletal and graphic textures are common, but pure grains are also present. One difference found in these two samples, is that P7 Bt horizon sample presents magnetite crystals smaller than 1 μm, which are absent in P7 C horizon sample. These small grains are more oxidized than larger grains (Figure 7).

Mineral magnetic concentration and grain size

The estimation of the relative magnetic concentration can be assessed from χ, ARM, SIRM, M_S, and M_R parameters. ARM is highly sensitive to grain size and concentration of ferrimagnetic minerals of single domain (SD) and small pseudo-single domain (PSD) grains (~0.1–1 μm) (Hunt *et al.*, 1995).

χ, ARM, SIRM, M_S, and M_R, all display similar patterns of variation in a depth profile (Figure 8). The older, Red paleosols P7 and P6 have the highest concentration of ferrimagnetic minerals. χ is >5 mm³/kg, ARM is mostly >0.1 mAm²/kg, and SIRM >3 mAm²/kg. Paleosols P2 and P1 have the lowest concentrations, with χ<1 mm³/kg, ARM <0.01 mAm²/kg, and SIRM <0.5 mAm²/kg. Modern soil S1 and Brown set paleosols P5, P4 and P3 have similar concentration values, intermediate between the two extreme groups previously described.

ARM values, normalized by SIRM to correct for changes in concentration, are used to estimate the relative abundance of SD and PSD ferrimagnetic grains. Magnetic hysteresis-loop parameters plotted on a M_R/M_S *vs.* B_{CR}/B_C diagram are a guide of grain size (Day *et al.*, 1977). However, these parameters are also affected by mixtures of different grain sizes and different mineral magnetic phases with contrasting coercivity spectra. Consequently, the derived grain size estimation from rock magnetism parameters may not be sufficiently adequate when these mixtures are present.

Frequency dependence of susceptibility has commonly been used as an indicator of ultra-fine (<30 nm), superparamagnetic (SP) material. However, because it is

also dependent on Ti content in titanomagnetites (de Wall and Worm, 2000), interpretations of SP content from this parameter may only be valid when magnetite is the magnetic mineral. This inconvenience is solved by using χ/M_S ratio, which depends on the SP content.

M_R/M_S ratio points to large PSD and multidomain (MD) grains throughout the profile, while B_{CR}/B_C are near the boundary between PSD and MD grains. ARM/SIRM generally points to smaller PSD grains in P5, P6, and P7, based on their moderately higher values of this ratio. Except the modern soil (S1) and P2, which has no C horizon, all paleosols have relatively higher χ/M_S ratio values in Bt horizons than in their C horizons, suggesting higher SP grain content in Bt horizons.

Changes in the concentration of TiO_2, which is immobile in most post-depositional conditions and thus represent the primary content of heavy minerals in soils, shows a trend of variations similar to those observed in the concentration of ferrimagnetic minerals inferred from χ, ARM, SIRM, M_S, and M_R parameters (Figure 5). The highest values are found in P7 and P6 and the lowest in P1, although P5, P4 and P3 paleosols have only slightly lower values than P7 and P6. An opposite variation is observed in P2 samples, as they peak while ferrimagnetics decrease. Fe_2O_3 is considered to be stable under subaerial weathering concentration (Pye, 1987), but it is removed under reducing conditions. Iron oxides closely follow the variations of TiO_2, but differ in two maxima in Bt horizon of P3 and in the upper samples of P1.

DISCUSSION

The three sets of paleosols show, in general terms, different combinations of mineral magnetic characteristics.

Ti-magnetites were directly observed in P7 by SEM and RLM. TiO_2 content values for P6, P5, P4, P3, and P2 paleosols, similar to those of P7, and Curie temperature estimations of magnetic mineralogy, support the assumption that Ti-magnetites are the main ferrimagnetic minerals in these paleosols. Hematite grains and hematized Ti-magnetites, were also observed in P7 samples by RLM. Curie temperature estimations possibly suggest the presence of hematite in P7, P6, P2, and P1 paleosols and in the modern soil S1. B_{CR} and S ratios indicate the presence of a high coercivity phase in P2, P1, and S1. The presence of goethite has not been confirmed by any non-magnetic method.

From the rock magnetism parameters, the Red set paleosols (P7 and P6) have the highest content of ferrimagnetic minerals. TiO_2 and Fe_2O_3 concentrations are also the highest for the Red set paleosols (Figure 5). The Brown set paleosols (P5, P4, and P3) generally have lower concentration of ferrimagnetic grains and lower TiO_2 and

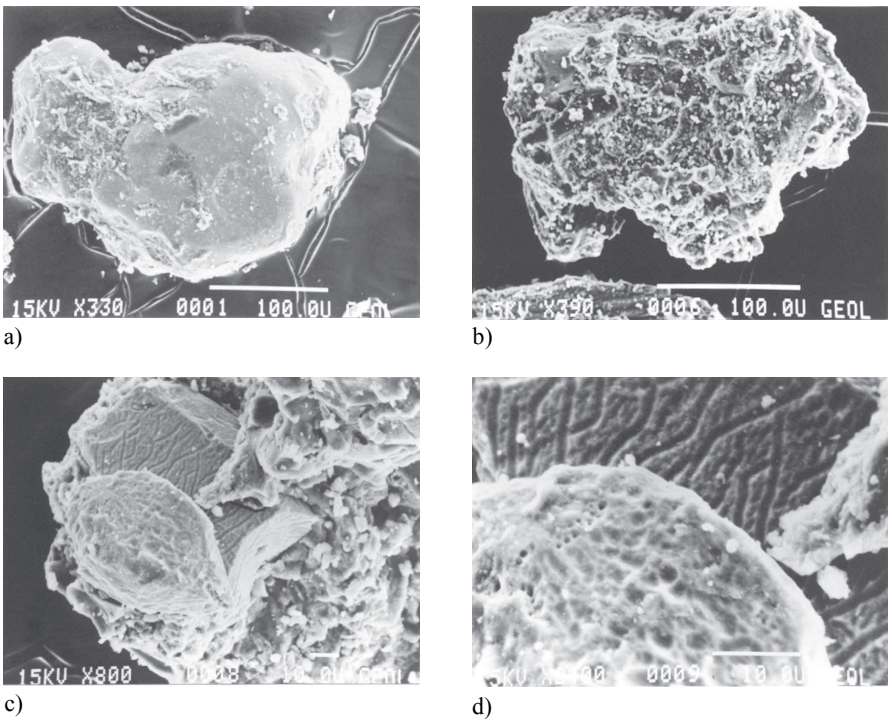

a) b) c) d)

Figure 6. Scanning electron microscopy of magnetic mineral grains from the paleosol P7. a) Fresh ilmenite grain with smooth surface from C horizon (330 X). b) Weathered ilmenite grain with corroded surface from Bt horizon (390 X). c) Two crystals of Ti-magnetite with etch pits on the surface from Bt horizon (800 X). d) Detail of (c) with higher magnification (2,400 X).

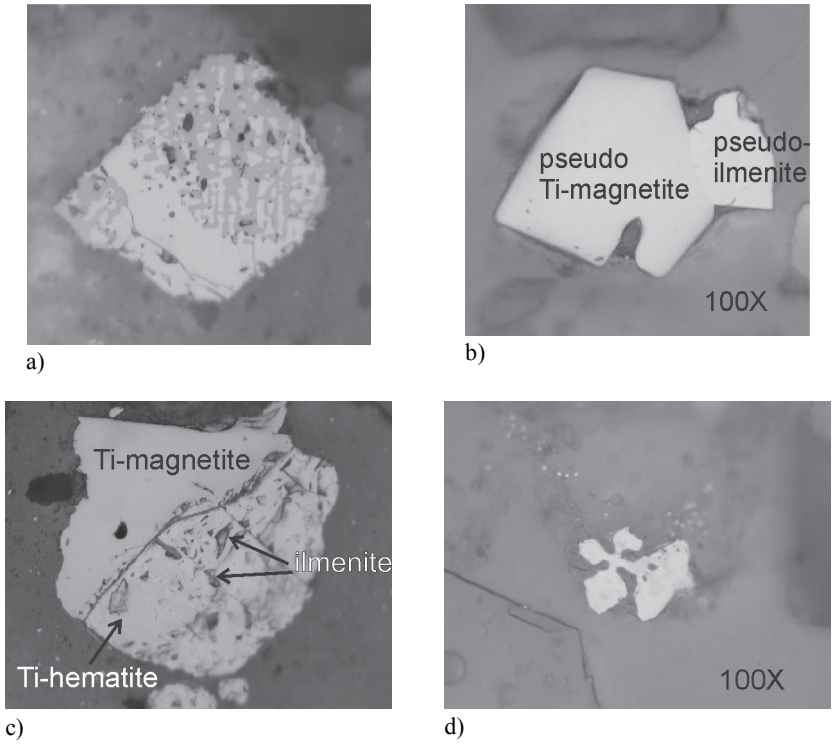

Figure 7. Reflected light microscopy images from paleosol P7. a) Ti-hematite and ilmenite intergrowths, with graphic texture, from Bt horizon (50 X). b) Subhedral Ti-magnetite grain intergrown with ilmenite from C horizon, both hematized. Ilmenite shows higher hematization (100 X). c) Grain with two sections: to the left is Ti-magnetite, to the right ilmenite partially replaced by Ti-hematite, from Bt horizon (50 X). d) Skeletal Ti-magnetite, from C horizon (100 X).

Fe_2O_3 concentrations than the Red set. However, the Bt horizon of P5 has similar values of the two oxides as the Red set, and also has the lowest χ of all Red and Brown set paleosols. Paramagnetic contribution to χ, χ_p, is higher in the Bt horizon of P5 (Figure 5), and also S ratios values are slightly lower for the same horizon. These characteristics could indicate that weathering processes have affected P5 paleosol more strongly than in P4 and P3, which have resulted in the increase of TiO_2, and the formation of paramagnetic and antiferromagnetic (hematite) minerals.

A grain size characterization based on magnetic parameters is uncertain given the mixtures of mineral phases. However, some interpretations can be made. The hysteresis parameters ratio M_R/M_S points to coarse, MD grains throughout the sequence. B_{CR}/B_C and M_R/M_S values of the Bt horizon of P4 point to coarser grains. ARM/SIRM ratio suggests the presence of smaller ferrimagnetic grains in Bt horizons of P7 and P5.

In addition to Ti-magnetites, small pure magnetite grains (~1 mm) were also observed in P7 Bt horizon. Magnetite may be of magmatic origin, or secondary as a result of pedogenic processes. The pedogenic magnetite is commonly characterized by a fine-grain size, as previously discussed. χ/M_S, which is a reliable indicator of ultrafine SP particles, occur in higher values in Bt horizons relative to the corresponding C horizons in paleosols of the Red and Brown sets. In many soils, higher concentrations of magnetic minerals than those of the parent material have been found (Mullins, 1977; Özdemir and Banerjee, 1982; Heller and Liu, 1982, 1984). This phenomenon, called "magnetic enhancement", is commonly caused by an accumulation of fine to ultra-fine-grained maghemite or magnetite. According to the χ/M_S values, magnetic enhancement may be present in Red and Brown set paleosols of Barranca Tlalpan. $\chi_{fd\%}$ values, which are not conclusive about the SP grain content where variable Ti titanomagnetites are present, also point to higher concentration of SP grains in Bt horizons of the Red set. The corroded surfaces observed on ilmenites and Ti-magnetites from Bt horizon samples of P7 (Figure 6), indicates that dissolution of these minerals has occurred. A later product of this process could be the neoformation of the pure, small magnetite grains observed in the Bt horizon of P7.

The Gray set paleosols (P2 and P1) and the modern soil (S1) have different characteristics than the older sequences. The more complex χ *vs.* high temperature behavior they exhibit, may be the result of a multi-component mineralogy, with several magnetic phases and high paramagnetic concentration. P2 displays characteristics that mark a transition between P3 and P1 in most mineral magnetic parameters. The modern soil (S1) has similar

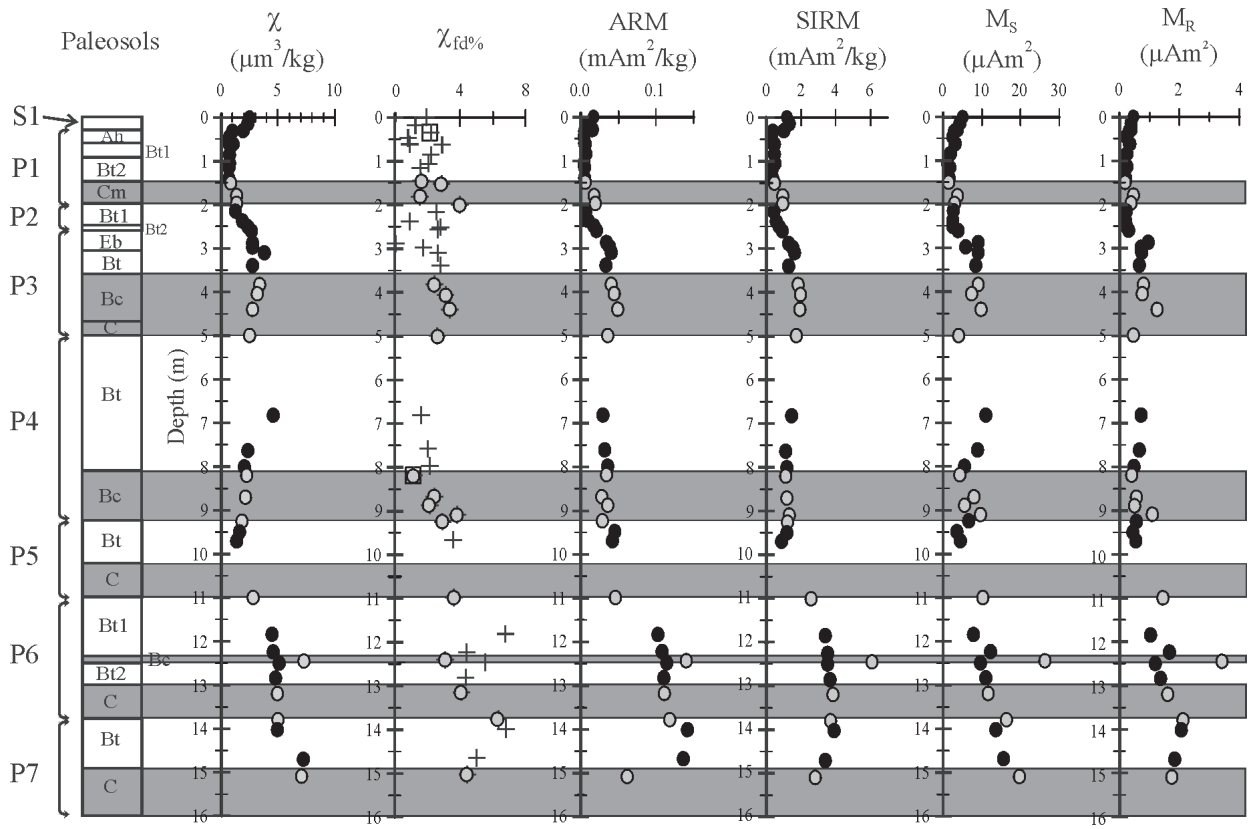

Figure 8. Depth profiles of mineral magnetic concentration parameters. χ: Bulk susceptibility, $\chi_{fd\%}$: frequency dependence of susceptibility, ARM: anhysteric remanent magnetization, SIRM and M_R: saturation of isothermal remanent magnetization, M_S: magnetization of saturation. Open symbols on gray shaded areas correspond to samples from BC and C horizons.

magnetic values as P2.

The paleosols from the Gray set show the lowest concentration of ferrimagnetic minerals. Peak values in TiO_2, Fe_2O_3 and in χ_p in P2 Bt1 horizon (Figure 5), suggest that weathering processes have been intense, leading to a concentration of these two oxides and iron paramagnetic minerals. The Cm horizon of P1 is the parent material that shows the lowest ferrimagnetic concentration and TiO_2 and Fe_2O_3 values of all the sequence. Similar low concentrations are also present in Bt2 and Bt1 horizons of P1. S ratios (Figure 4) and the ferrimagnetic contribution to susceptibility, χ_f (Figure 5), are also the lowest in the Cm and both Bt horizons. The Ah horizon of P1 has a sharp peak of paramagnetic contribution, χ_p, and Fe_2O_3 concentrations, while TiO_2 rises moderately. Even if the parent material of P1 paleosol originally had low ferrimagnetic mineral content, the decrease of Ti and Fe oxides, ferrimagnetic susceptibility, and S ratios, as well as the high B_{CR} values in the Bt horizons, indicate that intense weathering has affected this soil. Hematite or goethite content should be significant in these Bt horizons.

The obtained results allow us to formulate some preliminary hypotheses concerning the relation of paleosol magnetic characteristics to pedogenic processes and, on this basis, an approach towards their paleoenvironmental interpretation. The dominance of coarse size magnetic components and Ti-magnetites among them prove that primary volcanogenic magnetic minerals, to a large extent, determine the magnetic susceptibility values, both in sediments and in paleosols.

Is the process of pedogenic production of fine-grained magnetic minerals (which is supposed to cause χ value enhancement in loess-derived paleosols) detectable also in volcanic paleosols? An apparent characteristic increase of ultrafine ferrimagnetic grains in Bt horizons from the Red and Brown set paleosols does occur. More extensive sampling of both C and Bt horizons could confirm this preliminary observation. We assume that weathering of the volcanogenic magnetic components, in the course of soil formation, is responsible for the neoformation of ultrafine magnetite. However, in these paleosols, the indicators for ferrimagnetic concentration (χ, ARM, SIRM, M_S) do not show a clear enhancement in Bt horizons, which means that pedogenic neoformation has minor importance compared to the transformation of primary magnetic components. An alternative interpretation is that neoformed minerals are lost by a later reductive dissolution.

Intensive redoximorphic processes, clearly manifested

in the morphological features of Gray set paleosols, presented an additional factor of magnetic mineral destruction. The characteristics observed in the Gray set paleosols suggest that the paleosols formed in a permanently humid paleoclimate, and underwent the most aggressive environment affecting both volcanogenic and pedogenic magnetic components through intensive weathering and redoximorphic processes. A paleoclimate with seasonal precipitation contrast, under which the Red set paleosols are interpreted to be formed, is more suitable for pedogenic magnetic mineral accumulation and preservation.

However, in the Gray set paleosols P1 and P2, the ultrafine magnetic component expressed in the χ/M_S ratio and the content of hematite/goethite indicated by its high coercivity, are the highest in all the sequence. Both characteristics are in opposition to intensive redoximorphic processes, as they would preferably destroy the finer grains and the ferric (hematite/goethite) iron minerals. A possible explanation for this contradictory data is modern late-generation formation of hematite in these paleosols.

CONCLUSIONS

The magnetic properties allow us to distinguish among different types of paleosols. The results of rock magnetism analysis show that differences in magnetic parameters and morphological and chemical data found in this sequence of soil and paleosols are due to variations in the history of development of each paleosol, and not to differences between the processes in each soil horizon. Consequently, each paleosol reflects a particular history, despite the inherently common processes that occur in every soil horizon.

Paleosols from the Red and Brown sets, P7 and P6, and P5, P4, and P3, respectively, still conserve evidence of formation of ultrafine grains, probably derived from pedogenic processes operating in the Bt horizons. At least for the Red set, it can be considered that the magnetic enhancement may have occurred, and was partially destroyed by later processes.

ACKNOWLEDGEMENTS

L. Baños and T. Pi for XRD, R. Lozano for XRF; L. Rivas for RLM, G. Werner for field work assistance. We specially thank S. Banerjee and an anonymous reviewer for their fruitful comments. This work was partially founded by several sources: DGAPA PAPIIT IN107902 and IN104600, CONACyT G-28528T, 32337T and DLR MX00/014, and ICSU grant program for 2003, project "Polygenetic models for Pleistocene paleosols". The low temperature magnetic data were acquired at the University of Minnesota's Institute for Rock Magnetism (IRM). The IRM is also supported by the Instrumentation and Facilities program of the U.S. National Science Foundation (Earth Sciences Division).

REFERENCES

Bèget, J., 1990, Middle Wisconsinian climate fluctuations recorded in Central Alaska loess: Géographye physique et Quaternaire, 44(1), 3–13.

Birkeland, P.W., 1984, Soils and Geomorphology: New York, Oxford University Press, 372 p.

Birkeland, P.W., 1992, Quaternary soil chronosequences in various environments; extremely arid to humid tropical, *in* Martini, I.P., Chessworth, W. (eds.), Developments in Earth Surface Processes; 2, Weathering, Soils and Paleosols: The Netherlands, Elsevier Science Publishers B.V., 261–281

Day, R., Fuller, M., Schmidt, V.A., 1977, Hysteresis properties of titanomagnetites: grain-size and compositional dependence: Physics of the Earth and Planetary Interiors, 13, 260–267.

de Wall, H., Worm, H.U., 2000, A cautionary note on interpreting frequency-dependence of susceptibility solely in terms of superparamagnetism: University of Minnesota, Institute for Rock Magnetism Quarterly, 10(4), 1–6.

Dearing, J.A., Hay, K.L., Baban, S.M.J., Huddleston, A.S., Wellington, E.M.H., Loveland, P.J., 1996, Magnetic susceptibility of soil: an evaluation of conflicting theories using a national data set: Geophysical Journal International, 127, 728–734.

Dunlop, D.J., Özdemir, Ö., 1997, Rock magnetism, fundamentals and frontiers: New York, Cambridge University Press, 573 p.

Fassbinder, J.W.E., Stanjek, H., Vali, H., 1990, Occurrence of magnetic bacteria in soil: Nature, 343, 161–163.

Heller, F., Liu, T.S., 1982, Magneostratigraphical dating of loess deposits in China: Nature, 300, 431–433.

Heller, F., Liu, T.S., 1984, Magnetism of Chinesse loess deposits: Geophysical Journal of the Royal Astronimical Society, 77, 125–14

Hunt, C.P., Moskowitz, B.M., Banerjee, S.K., 1995, Magnetic properties of rocks and minerals, *in* Ahrens, T.J.(ed.), Rock physics and phase relations, a handbook of physical constants: American Geophysical Union, Reference Shelf Series, 3, 189–204.

Kletetschka, G., Banerjee, S.K., 1995, Magnetic Stratigraphy of Chinese loess as a record of natural fires: Geophysical Research Letters, 22 (11), 1241–1343.

Kukla, G., 1988, The mystery of the Chinese magnetic dust: Palisades NY, Lamont-Doherty Geological Observatory, Yearbook.

le Borgne, E., 1960, Influence du feu sur les propriétés magnétique du sol et sur celles du schiste et du granit: Annales de Geophysique, 16, 159–195.

Lovely, D.R., Phillips, E.J.P., 1986, Organic matter mineralization with reduction of ferric iron in anaerobic sediments: Applied Environmental Microbiology, 51, 683–689.

Maher, B.A., Thompson, R., 1991, Mineral magnetic record of the Chinese loess and paleosols: Geology, 19, 3–6.

Maher, B.A., Thompson, R., 1995, Paleorainfall reconstructions from pedogenic magnetic susceptibility variations in the Chinese loess and paleosols: Quaternary Research, 44, 383–391.

Mullins, C.E., 1977, Magnetic susceptibility of the soil and its significance in soil science - a review: Journal of Soil Science, 28, 223–246.

Oches, E.A., Banerjee, S.K., 1996, Rock magnetic proxies of climate change from loess-paleosol sediments of the Czech Republic: Studia Geophysica et Geodaetica, 40, 287–300.

Özdemir, O., Banerjee, S.K., 1982, A preliminary magetic study of soil samples from west-central Minnesota: Earth and Planetary Science Letters, 59, 393–403.

Özdemir, Ö., Dunlop, D.J., Moskowitz, B.M., 1993, The effect of oxidation on the Verwey transition in magnetite: Geophysical Research Letters, 20, 1671–1674.

Pye, K., 1987, Aeolian dust and dust deposition: London, Academic Press, 334 p.

Reynolds, R.L., King, J.W., 1995, Magnetic records of climatic change: Reviews of Geophysics, 33 (suplement), 101–110.

Sedov, S., Solleiro-Rebolledo, E., Gama-Castro, J.E., Vallejo-Gómez, E., González-Velázquez, A., 2001, Buried palaeosols of the Nevado de Toluca: an alternative record of Late Quaternary environmental change in central Mexico: Journal of Quaternary Science, 16(4), 375–389.

Singer, M.J., Fine, P., 1989, Pedogenic factors affecting magnetic susceptibility of northern California soils: Soil Science Society of America Journal, 53, 1119–1127.

Stanjek, H., Fassbinder, J.W.E., Vali, H., Wagele, H., Graf, W., 1994, Evidence of biogenic greigite (ferrimagnetic Fe_3S_4) in soil: European Journal of Soil Science, 45, 97–104.

Thompson, R., Oldfield, F., 1986, Environmental magnetism: London, Allen and Unwin, 227 p.

Manuscript received: October 24, 2002
Corrected manuscript received: November 18, 2003
Manuscript accepted: December 17, 2003